D.P. Report 358
AERE - R 4994

DRAGON PROJECT USE ONLY

D.P. Report 358
AERE - R 4994

O.E.C.D. HIGH TEMPERATURE REACTOR PROJECT

DRAGON

Dragon Project Report

DIFFUSION OF BARIUM, STRONTIUM AND CERIUM IN VARIOUS GRADES OF REACTOR GRAPHITE

R. L. FAIRCLOTH F. C. W. PUMMERY B. A. ROLLS

Chemistry Division,

Atomic Energy Research Establishment,

Harwell, Berkshire.

July 1965

UNCLASSIFIED
(Approved for Publication)

AERE - R 4994
DPR 358

DIFFUSION OF BARIUM, STRONTIUM AND CERIUM IN VARIOUS GRADES OF REACTOR GRAPHITE

by

R. L. Faircloth

F. C. W. Pummery

B. A. Rolls

Chemistry Division,
U.K.A.E.A. Research Group,
Atomic Energy Research Establishment,
HARWELL.

July, 1965.

HL.65/3722 (C.14)

1. Introduction

A knowledge of the rate and mechanism of the migration of metallic fission products through graphite is of importance in the design of high temperature reactor systems, such as Dragon, where graphite is used for fission product containment. This paper describes an investigation, carried out as part of the Dragon Reactor Experiment Basic Research Programme, on the diffusion of barium, strontium and cerium through various grades of graphite of particular interest to Dragon.

2. Diffusion of Barium and Strontium in CYX165, G5 and HX30 Graphites and Pyrographite

2.1 Experimental Technique

In these experiments small specimens of graphite in the form of blocks or cylinders were prepared such that there was at least one highly polished flat face serving as a base line for diffusion measurements. The polishing was carried out on emery polishing papers, down to grade 4/0, supported on a flat glass plate. The specimens were then exposed, in sealed evacuated tubes, to the vapour of either barium or strontium metal under controlled conditions of temperature and pressure for known periods of time.

For experiments below 1000°C stainless steel tubes of 0.014 in wall thickness were used as the containment vessels. The loading operations were performed in an argon atmosphere dry-box to minimise corrosion of the reactive fission product metals, about 1 gram of metal being placed in the bottom of each tube and the graphite specimens, in molybdenum cups, near the top. The tubes were then closed with a cap of 0.008 in thick stainless steel painted with a high temperature brazing alloy (Endewrance CM60) suspended in an acetone-collodian mixture. Each assembly was loaded into a glass sealing apparatus which was closed, removed from the dry-box, and attached to a vacuum line. After pumping for some hours the upper part of the stainless steel tube was inductively heated at just below the brazing temperature to facilitate out-gassing of the graphite specimen whilst the lower part was cooled by liquid nitrogen to inhibit volatilisation of the barium or strontium metal. When a pressure of less than 1 micron had been achieved the temperature was raised sufficiently for brazing of the lid to the body of the tube to occur. The induction heating was stopped and after allowing the tube to cool it was removed from the sealing apparatus and the seal checked visually. The tube was then loaded into a resistance furnace wound with two independent heating coils, the complete assembly being shown in Fig. 1.

The graphite temperature was monitored by a thermocouple fitted into a small tube which also formed the support for the molybdenum cup containing

the specimen whilst the temperature of the volatile metal was measured by a second thermocouple fitted into a cavity at the bottom of the stainless steel tube. Pt-Pt/10%Rh thermocouples were used throughout.

Stabilised power was then fed, from "Variacs", into the two independently wound heating coils to maintain a constant temperature gradient across the stainless steel tube, conditions always being chosen to make the graphite temperature higher than that of the volatile metal. During each run the upper and lower temperatures were constantly monitored and maintained to $\pm 2^{\circ}C$ in most cases. In this way soakings of numerous graphite specimens at various known temperatures in controllable pressures of either strontium or barium vapours could be achieved. Each soaking was carried out under conditions where heating and cooling times could be neglected when compared with the actual soaking time. In particular the cooling time was made extremely small by rapid removal of the soaking tube from the furnace at the termination of each run and immersing it first in water and then in liquid nitrogen.

Although most of the experiments carried out so far have been at below $1000^{\circ}C$ an experimental technique has been developed for operation between $1000^{\circ}C$ and $1500^{\circ}C$ and this will be briefly described. A molybdenum soaking tube was used and after loading with the specimen and metal the top was covered with a 0.005" thick ring of zirconium, followed by a 0.010" thick disc of molybdenum, the whole being strapped tightly in position with 0.020" diameter tantalum wire. The tube was then placed in the glass sealing apparatus and was evacuated as before. After preliminary heating of the upper part of the molybdenum tube for out-gassing purposes the temperature was raised rapidly to melt the zirconium washer at which point heating was terminated. Thermocouples were spark welded onto the side of the sealed tube at two positions close to the graphite specimen, and the tube was then placed in the high temperature soaking apparatus shown in Fig. 2. In this apparatus the molybdenum tube was heated at the top by an induction coil the lower, bottom, temperature being maintained by conduction. The actual temperature of the graphite as related to the outer thermocuple readings, coil position and furnace settings was deduced from previous calibration experiments. For these an open molybdenum tube was used with a black body in place of a graphite specimen. The readings of the thermocouples were compared with pyrometer readings for several portions of various coils and also in the presence or absence of heat shields on the lower part of the molybdenum tube.

At the conclusion of each soaking experiment the lid of the cooled tube was pierced and the specimen removed. Approximately half the specimen

was then removed, by grinding and polishing so as to give a highly polished face at right angles to the original reference plane. The concentration profile of the fission product metal along the centre of this face and perpendicular to the reference plane was then determined by electron probe micro-analysis using a "Cameca" microprobe of approximately $1\mu^2$ probe area.

2.2 Results and Discussion

2.2.1 CYX165 Graphite

Specimens for experiments with this material were taken from a piece of Pluto 4 fuel tube. This graphite, Dragon Grade 9 (impregnated) was produced in the baked form by Morganite Carbon Ltd. who designated it CYX165. It was then subjected to a double impregnation with furfuryl alcohol followed by baking and high temperature degassing. Due to carbon deposits within the network from these impregnations the diffusion of rare gas fission products is reduced to an acceptable level for use as a containment material in Dragon. The high value for the surface area (believed to be $\sim$ 3-5 m^2/g)[1] may be attributed to this deposited carbon in the pores. The density is $\sim$ 1.70 g/cm^3 and the pore size distribution curve shows that the majority of pores have entrance diameters of less than 1μ [2].

Diffusion experiments were carried out with both barium and strontium and a typical microprobe recording for each of these, along with the experimental conditions, is shown in Fig. 3 and Fig. 4 respectively. It is immediately obvious from these recordings that the smooth concentration profiles which would arise from a simple case of bulk diffusion do not obtain in this case. Instead points of high concentration occur (which presumably represent pores, grain boundaries, and other defects) with regions of very low concentration between them indicating a relatively small in-grain diffusion contribution. The peak height generally decreases with increasing distance from the reference surface and eventually the trace becomes indistinguishable from the instrumental background. Thus, diffusion of metal from the sides of the specimen (other than the reference surface) does not, in these cases, contribute to the profile so that the problem reduces to one of diffusion from a plane surface at which the solute metal concentration is constant (i.e. constant vapour pressure) into a semi-infinite solid. In order to calculate an apparent diffusion coefficient an integration procedure was carried out on each microprobe trace to determine the variation of the average solute metal concentration with penetration distance. The concentration profiles thus obtained were then fitted by computer to the best error function relationship, i.e.

$$C = C_o \left[1 - \operatorname{erf} \frac{x}{2\sqrt{Dt}}\right]$$

where C is the solute metal concentration at distance x cm from the surface, C_o is the concentration at the surface ($x = o$), t is the time (seconds) and D the diffusion coefficient ($cm^2 s^{-1}$).

The results for all the barium experiments with CYX165 graphite are shown in Table I, together with the relevant experimental conditions and the results for strontium diffusion are similarly given in Table II. Arrhenius plots for this data are shown in Fig. 5 from which activation energies of 32 ± 4 kcal/mole and 31 ± 3 kcal/mole for barium and strontium diffusion respectively are obtained. These represent weighted least squares fits to the data, the weights depending on the goodness-of-fit of each experimental profile to the "best" error function.

The fact that these activation energy values are considerably smaller than would be expected for in-grain diffusion in graphite indicates clearly that activated surface diffusion in defects in the graphite matrix is the dominating mode of mass transfer, a fact which is substantiated by the general form of the microprobe traces.

Since the microprobe could not be used to give a quantitative estimate of the solute concentration, the concentration axis of a microprobe trace could only be calculated in arbitrary units. To overcome this difficulty the specimen arising from one of the barium soaking experiments (barium in CYX165 No.3), which was in the form of a half-cylinder, was further ground and polished, such that all the graphite containing barium which had diffused in other than from the original reference face was removed. The concentration of the barium in the residual right angled block was then determined by neutron activation analysis. The surface area of the reference surface was measured giving the quantity of barium which had diffused in per unit area of surface. The smoothed profile having been normalised to this quantity the surface concentration was calculated as ~ 60 mg of barium/g of graphite. This serves, at least semi-quantitatively, to indicate the concentration range in which the experiments described here belong.

No investigation has been made at this time to study the possible dependence of apparent diffusion coefficient on the concentration of the diffusing species. It may however be implied from the results of other workers that a decrease in concentration produces a marked change in diffusion coefficients and activation energies to a level where the values become comparable to those expected for true bulk diffusion. It seems probable that at a concentration of solute atoms below that required to form a monolayer (say ~ 1 mg/g) surface diffusion might be controlled by rupture of metal-graphite bonds at the surface. The bonding of successive

layers beyond a monolayer would tend towards the physical rather than the chemical in nature and a decrease in the activation energy for diffusion would follow.

It should be noted that the diffusion coefficients obtained by the procedure are only nominal values and cannot be related directly to grain boundary diffusion coefficients. The idealised problem of diffusion in solids containing grain boundaries has been studied by Fisher[3] and further by Whipple[4]. These treatments have been discussed by Wood et al[5] and applied to grain boundary diffusion of gold in copper by Austin and Richard[6] and to grain boundary and lattice diffusion of chromium in zinc by Agarwala[7]. Unfortunately it has not yet been found possible to apply these idealised solutions to the case at present under investigation. When grain boundary diffusion is the over-riding form of mass transfer the diffusion profiles should be such as to give a linear log concentration versus distance plot, from which the grain boundary diffusion coefficient can be derived with knowledge of the lattice diffusion coefficient and the grain boundary width. The present data cannot be so represented.

It is, however, of interest to note that the profiles can be fitted to a log concentration versus $(\text{distance})^2$ line. From a least squares analysis a statistically justifiable fit was obtained in all the cases examined. Assuming that the concentration-distance relationships is of the form

$$C = C_o \exp\left(-\frac{x^2}{4Dt}\right)$$

values of D for barium diffusion were calculated. These values are included in Table I and were lower than from error function fitting but provided a rather better Arrhenius plot with an activation energy of 35.0 ± 0.5 k cal/mole. However it should be noted that this solution refers to diffusion from a thin, non-renewed film rather than to that from a constant source.

2.2.2 G5 Graphite

Barium diffusion experiments have been carried out at approximately 750°C, 850°C and 950°C with specimens of G5 graphite taken from both Pluto 5 and Pluto 6 fuel tubes.

The pore structure of G5 graphite is very different from that of CYX165; in particular, while an appreciable number of pores with entrance diameter 0.015 to 0.2μ are observed the pore size distribution curve peaks at 1.5 to 4.0μ[8]. In this case the theoretical porosity approaches 30% and the density is 1.58 g/cm^3. The surface area is believed to be 0.3 to 0.5 m^2/g, the pores not being filled with resin carbon.

A typical micrprobe recording is shown in Fig. 6 along with the relevant experimental conditions. Neutron activation analysis has again been used to

approximately calibrate the vertical scale of this recording. The profiles obtained with the electron microprobe show two distinct features:-

(a) A series of peaks, starting from the reference plane, similar to those observed with CYX165 graphite, but decreasing in size much more rapidly with increasing penetration distance, and

(b) a long, irregular (but generally diminishing with increasing penetration distance) "tail" which extends far into the specimen only slightly greater than the detection limit of the instrument.

Fitting error functions to these profiles appears to give diffusion coefficients very much smaller than those for comparable conditions in CYX165. This is, however, misleading when applied to the mass transfer of barium through this type of graphite as the fit does not take account of the long "tail" mentioned above. In other words, adequate fitting of the experimental profiles to single error functions is not possible.

Neutron activation analysis of sections of two of the soaked G5 specimens (Nos. 27 and 28) indicated that the average solute concentration over the diffusion "tails" was approximately 13 mg barium/g graphite in each case, the detection limit of the microprobe being approximately 5 mg/g. An accurate analysis of the shape of this part of the diffusion profile is obviously not possible under these circumstances but an approximate value for the diffusion coefficient in the "tail" has been obtained in one instance. This result along with apparent diffusion coefficients derived from the initial part of each profile are summarised in Table III along with the experimental conditions in each case.

The steep, irregular "leading edge" profile observed in all the G5 experiments is almost certainly associated with compound formation and the concomitant production of large-scale structural damage in the surface region. This is supported by the optical appearance of those regions which give large responses on the microprobe. These generally arise from obvious defects which generate directly from the specimen surface or from areas of different optical appearance from the graphite matrix which may be a second phase. These latter are only visible within a few microns of the edge of the specimen.

It seems probable that the predominant mode of mass transfer of solute metal in G5 graphite, as in CYX165, is via structural defects. In the absence of resin carbon, however, the capacity of the defects for barium is much smaller, with the result that the prominent peaks of high concentration is CYX165 profiles are not seen in the case of G5 graphite, where the barium concentration over the majority of the profile is close to the limit of detectability.

2.2.3 HX30 Graphite

This graphite, manufactured by the Chemical Engineering Division at Harwell, represents an attempt to prepare a material with a narrow pore size distribution and good back-sweeping characteristics. Most of the pores in HX30 have an entrance diameter of 5 to 10μ.

The barium soaking experiments so far carried out with HX30 graphite at 761°C, 858°C and 902°C give "leading edge" diffusion coefficients of 7.4×10^{-10}, 4.7×10^{-9} and 1.0×10^{-8} cm^2/s respectively. The general shape of the profiles (for an example see Fig. 7) resembles those obtained with G5 graphite, in particular the existence of long diffusion "tails" is indicated, but with less prominent "leading edge" peaks. In addition high barium concentration spots were found to occur at random across the specimen surface. Correlation of these spots with simultaneous optical microscopy indicated that these were associated with pores with entrance diameters in the region of 5-10μ. In the case of some pores, the brilliant visible fluorescent usually connected with points of high barium concentration was observed, but with no response on the microprobe counter.

Soakings of HX30 graphite with strontium vapour under comparable conditions of temperature and pressure showed the same general pattern of behaviour as encountered in the work with barium.

2.2.4 Pyrographite

Only a few barium diffusion experiments have been carried out with pyrographite but with interesting results. With as-formed pyrographite long diffusion "tails" reminiscent of those found with G5 and HX30 graphites were observed in both the "a" and "c" directions, an example of an "a" direction profile being shown in Fig. 8. Experiments carried out at 762°C and 908°C gave apparent diffusion coefficients in the "a" direction of 1.0×10^{-6} and 1.4×10^{-5} cm^2s^{-1} respectively, figures which must be regarded as only approximate since the concentrations were only just above the instrumental detection limit. Penetration distances in the "c" direction were observed to be between one and two orders of magnitude smaller than in the "a" direction under comparable soaking conditions.

The profiles show a regular decrease of concentration with increasing penetration with no evidence for the existence of localised high concentration regions. It may be concluded, therefore, that diffusion in the "a" direction in pyrographite occurs by the same mechanism as diffusion in

well-graphitized polycrystalline graphite, namely along defects such as grain boundaries and micro-cracks.

The mechanism of diffusion in the "c" direction is not at present clear, but it appears likely that the easy diffusion path is along the cone boundaries with sideways movement into defects parallel to the "a" direction. These defects would obviously be filled much more slowly than if diffusion were from the "a" direction due to the smaller proportion of access points in the "c" surface.

The effect of high temperature annealing on the structure of pyrographite is now fairly well understood: the material attains a more perfect crystalline state with a decrease in the concentration of defects and an increase in inter-crystalline orientation. A decrease in the diffusion coefficients for impurity atoms does not necessarily follow although a marked decrease in the rate of mass transfer is to be expected from the decrease in available diffusion paths.

Two barium diffusion experiments have been carried out with pyrographite annealed at 2700°C. In the soaking at 766°C no penetration was detected in the "a" or "c" directions with the microprobe. In the soaking at 940°C, despite actual mechanical breakdown of the specimen no penetration could be observed in the "c" direction. In the "a" direction the microprobe trace showed a series of peaks over the first few hundred microns of the specimen with signs of a "tail" extending much further.

3. Diffusion of Cerium in HX30 Graphite

3.1 Experimental Technique

In these experiments a molybdenum cell, 2.0 cm in diameter and 3.5 cm long was used as the containment vessel. Cerium metal was placed at the bottom of the cell and the graphite specimen in the form of a cylinder 1.0 cm in length and 1.0 cm in diameter with one face polished accurately at right angles to its long axis was supported, polished face downwards, on a flange situated about 1.0 cm above the bottom of the cell. The cell was closed with a screw-threaded lid which pressed the graphite specimen firmly down onto the flange. The whole assembly, suitably supported on tungsten legs in a vacuum system, was heated inductively for a known period of time the temperature being measured by optical pyrometer observations, through a calibrated window/prism combination, of a black body hole in the top of the lid.

At the completion of each soaking experiment the cell was opened and the specimen extracted. The thin layer of cerium carbide which formed on the surface of the specimen was allowed to react with the atmosphere for some hours after which it could easily be removed. A core, 0.5 cm in

diameter and extending approximately 0.8 cm from the reference face, was removed from the centre of the specimen using a core-drill and parting-off tool mounted in a precision micro-lathe.

The core prepared in this manner was next irradiated in the Harwell reactor BEPO for periods of up to one hour along with a cerium standard and an untreated sample of HX30 graphite to serve as a blank. Cerium analysis was then carried out by counting the 0.145 MeV peak of the 33.1 day half-life Ce^{141} isotope produced in the irradiation. To determine the cerium distribution the specimen was cemented into the specimen holder of the sectioning apparatus shown in Fig. 9 taking great care to ensure that the surface of the specimen was correctly aligned with the plane of the polishing surface. After the specimen was correctly positioned in the holder its total activity was determined and this was followed by removal of successive sections of known thickness and re-determination of the total activity remaining at each stage. For each counting operation the specimen and holder were removed from the barrel of the sectioning apparatus and were weighed also, so that a cross-check between weight-loss and the corresponding section thickness was obtained.

These results were then recorded as the variation of F with x where

$$F = \frac{\text{activity remaining beyond } x \text{ cm}}{\text{activity of whole specimen}}$$

If the concentration profile is of an error function form then

$$F = \frac{\int_{\infty}^{\infty} \varepsilon \ \text{erfc}\ \varepsilon \ . \ d\varepsilon}{\int_{0}^{\infty} \text{erfc}\ \varepsilon \ . \ d\varepsilon}$$

where ε is the dimensionless variable $x/2\sqrt{Dt}$. Computed values of ε and F are given in Table IV.

From each experimentally determined value of F, a value of D may be determined since both x and t are known.

The distribution of cerium in the specimen could alternatively be determined directly by taking the difference between two successive counts and, by comparison with the standard and a knowledge of the weight of graphite removed, obtaining data for the cerium concentration in each specimen. This technique was used on a few sections of each specimen to establish the cerium concentration level but was not employed to obtain a complete concentration profile because of the increased errors necessarily arising in measuring differences amounting to only a few per cent of the total counts. It was also possible to count the emery paper after each

polishing operation but in general the activity levels were such that long counting times were necessary for satisfactory counting statistics to be obtained.

3.2 Results and Discussion

If the concentration profile in the specimen is of an error function from the values of diffusion coefficient obtained for any one experiment by the analysis described above should be constant to within the experimental error. In these experiments, however, it has been found that the calculated values of D show a downward trend with increasing penetration distance with the extent of the trend being as much as a factor of 4 in the worst case. In order to compare the results obtained at different temperatures and soaking times the values of D obtained in each experiment have been averaged and these, along with the highest and lowest values to demonstrate the extent of the trend and also the experimental conditions, are shown in Table V.

Smooth plots of fractional activity remaining (F) versus penetration distance were obtained in all the experiments and a typical example (from experiment number 4) is shown in Fig. 10. In each case, however, these plots are more linear than those calculated for an error function distribution indicating that the initial part of the concentration profile is showing a more uniform distribution of diffusing metal than would be expected from the appropriate diffusion laws. For purposes of comparison the theoretical curve obtained for the average diffusion coefficient derived for experiment 4 is included in Fig. 10, where the difference in shape between the two curves is clearly seen.

It is of interest to note that the concentration of cerium on the specimen surface (i.e. at $x=o$) was found to be close to 2 mg cerium/g of graphite in each case, a figure which is close to that expected for monolayer formation.

The variation of the averaged diffusion coefficients as a function of temperature is shown as an Arrhenius plot in Fig. 11 from which an activation energy for the diffusion process of 48 k cal/mole is obtained. It may be seen from this plot, and also from Table V, that the D values obtained at close to 1540°C (experiment Nos. 4, 5 and 6) are in good agreement in spite of the widely varying soaking times, indicating clearly the dependence of penetration distance upon the square-root of the soaking time.

On the basis of these facts the following mechanism for the diffusion of cerium through graphite is proposed. Cerium atoms enter the defect structure of the graphite, collide with the walls of these defects and are

tightly bound on active trapping sites to form a monolayer. Further cerium atoms strike the already adsorbed atoms and are physically absorbed. Further movement then occurs either by evaporation or by surface migration until these atoms are themselves finally fixed on vacant trapping sites.

4. Summary

The diffusion of barium and strontium in CYX 165 and HX 30 graphites, and of barium in G5 graphite and pyrographite has been studied using an electron microprobe. A sectioning technique has been applied to the diffusion of cerium in HX30 graphite.

It has been concluded that the movement of these metals through well-formed polycrystalline graphite and pyrographite occurs by activated surface diffusion, combined possibly with vapour phase migration, through microstructural defects.

In graphite containing ungraphitised material the bulk of the mass transfer occurs along the surface of this component.

5. Acknowledgement

The authors are greatly indebted to Mrs. P.M. Martin of Metallurgy Division, Harwell, for carrying out the microprobe determinations.

6. References

1. L.W. Graham, Private communication
2. L.W. Graham et al, D.P. Report 40
3. J.C. Fisher. J.Appl.Phys., 22 (1951) 74
4. R.T.P. Whipple. Phil.Mag., 45 (1954) 1225
5. V.E. Wood, A.E. Austin and F.J. Milford. J.Appl.Phys., 33 (1962)3574
6. A.E. Austin and N.A. Richard. Ibid., 33 (1962) 3569
7. Agawala et al. AEEJ/CD/22 (1964)
8. L.W. Graham and M.S.T. Price. D.P. Report 146

TABLE I

Barium in CYX165

Expt.No.	Graphite Temp. °C	P_{Ba} (mm Hg)	t(sec)	D_{exp} $cm^2 s^{-1}$	D_{erf} $cm^2 s^{-1}$
6	767	0.06	23.220	5.03×10^{-8}	1.13×10^{-7}
4	853	0.38	25,200	1.91×10^{-7}	4.99×10^{-7}
30	859	0.08	25,200	not calculated	5.58×10^{-7}
3	912	0.37	8,400	3.46×10^{-7}	1.42×10^{-6}
5	959	0.92	8,400	4.92×10^{-7}	9.47×10^{-7}
7	1188	0.42	5,820	8.01×10^{-6}	1.11×10^{-5}

TABLE II

Strontium in CYX165

Expt,No.	Graphite Temp. °C	P_{Sr} (mm Hg)	t(sec)	D_{erf} $cm^2 s^{-1}$
1	753	0.17	23.400	3.7×10^{-8}
5	753	0.17	22,920	5.1×10^{-8}
4	848	0.19	10,980	2.4×10^{-7}
2	923	0.19	8,400	4.4×10^{-7}

TABLE III

A: Barium in G5 (Pluto 5)

Expt.No.	Graphite Temp. °C	P_{Ba} (mm Hg)	t(sec)	D_{erf} $cm^2 s^{-1}$	D_{erf} $cm^2 s^{-1}$
				Leading Edge	Tail
15	763	0.07	27,000	6.8×10^{-9}	*
12	850	0.24	27,000	8.7×10^{-10}	**
28	942	0.18	28,800	7.3×10^{-9}	**
B: Barium in G5 (Pluto 6)					
29	760	0.12	28,800	2.9×10^{-10}	*
13	855	0.26	27,000	1.7×10^{-11}	**
27	947	0.18	28,800	2.8×10^{-8}	1.2×10^{-6}

*Tail not detected
**Tail not calculated

TABLE IV

Table Showing the Variation of F with ε

ε	F
0.00	1.000
0.05	0.914
0.10	0.833
0.15	0.757
0.20	0.685
0.25	0.619
0.30	0.557
0.35	0.500
0.40	0.447
0.45	0.398
0.50	0.354
0.55	0.313
0.60	0.276
0.65	0.243
0.70	0.213
0.75	0.186
0.80	0.162
0.85	0.140
0.90	0.121
0.95	0.104
1.00	0.089
1.05	0.076
1.10	0.065
1.15	0.055
1.20	0.046

TABLE V

Cerium in HX30

Expt.No.	Temperature (°C)	Time (s)	D average (cm^2s^{-1})	D maximum (cm^2s^{-1})	D minimum (cm^2s^{-1})
1	1333	10,800	7.3×10^{-7}	8.4×10^{-7}	6.1×10^{-7}
2	1525	10,800	3.8×10^{-6}	5.0×10^{-6}	3.4×10^{-6}
3	1430	10,800	2.5×10^{-6}	4.6×10^{-6}	1.1×10^{-6}
4	1540	10,800	4.8×10^{-6}	6.7×10^{-6}	3.1×10^{-6}
5	1544	3,600	4.2×10^{-6}	6.7×10^{-6}	1.8×10^{-6}
6	1542	32,400	5.0×10^{-6}	6.9×10^{-6}	4.1×10^{-6}

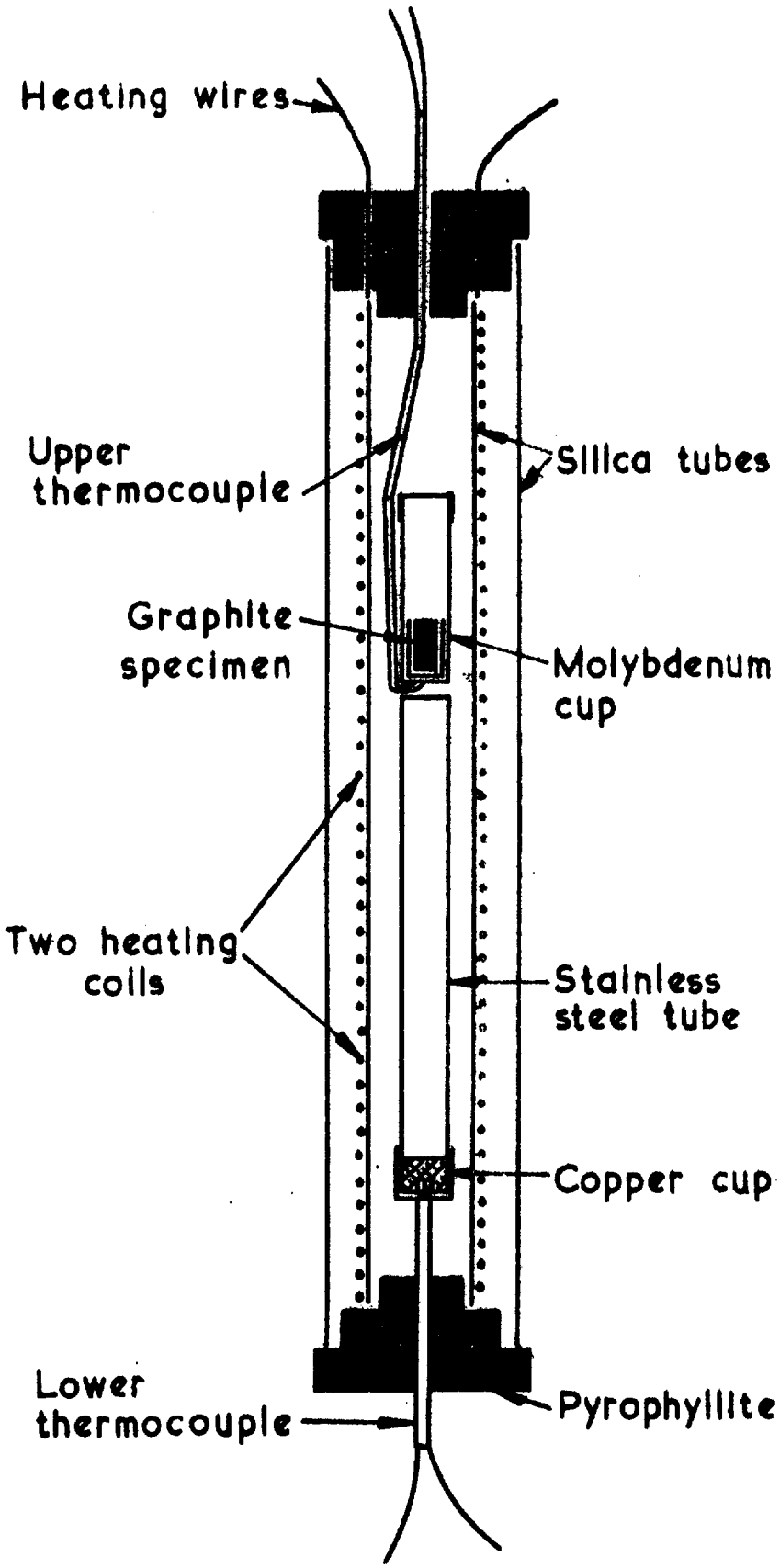

FIG.1 LOW TEMPERATURE SOAKING APPARATUS

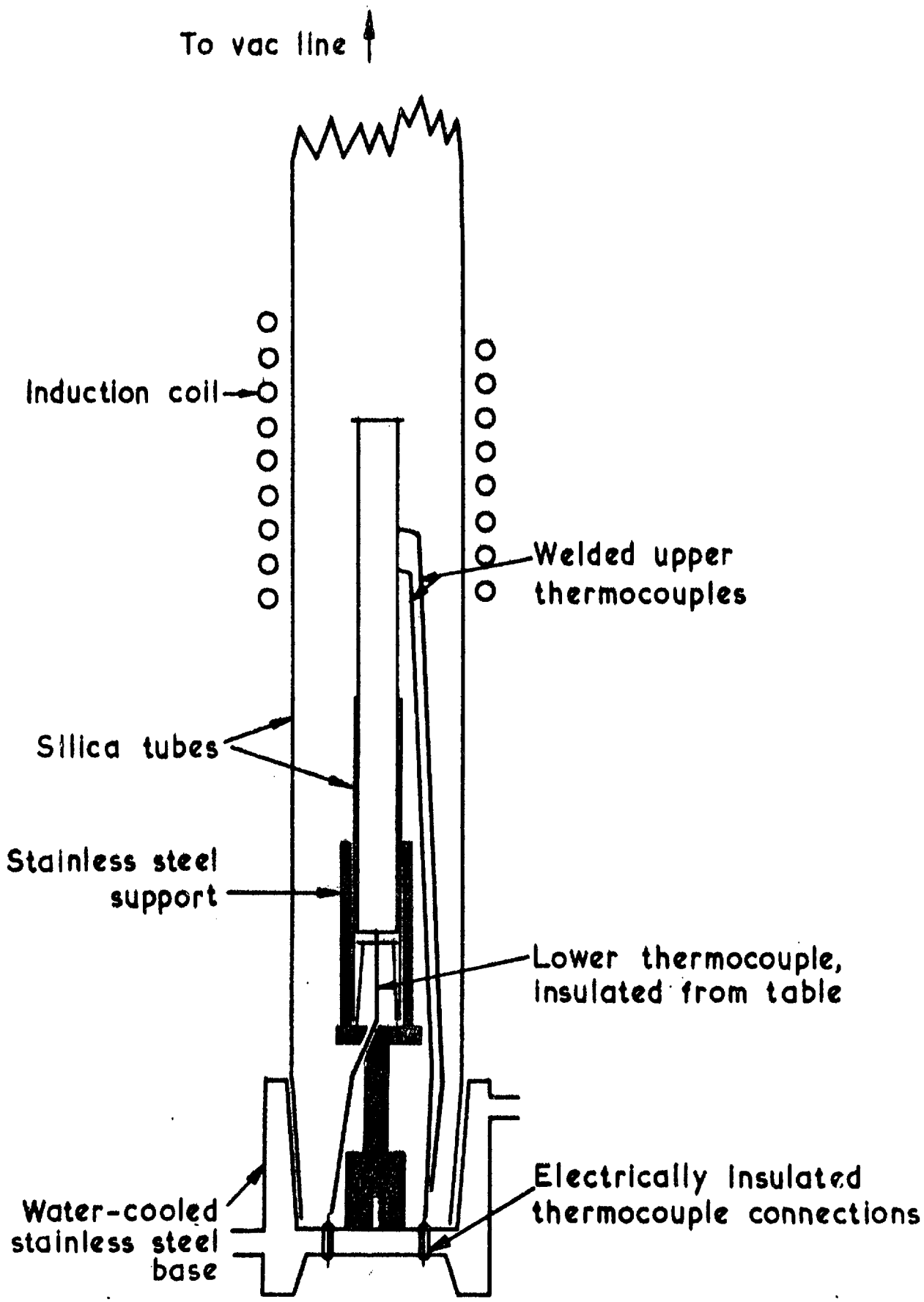

FIG. 2. HIGH TEMPERATURE SOAKING APPARATUS

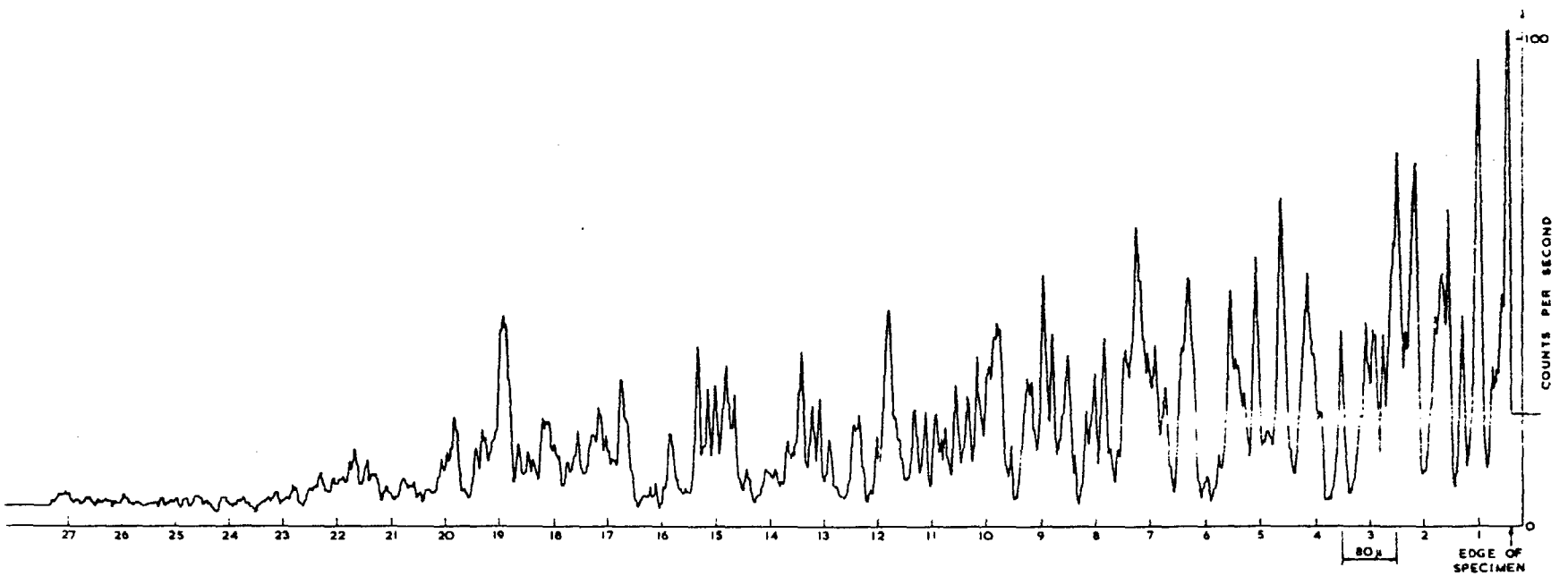

Fig 3

Microprobe recording for barium in CYX 165 graphite at 859°C

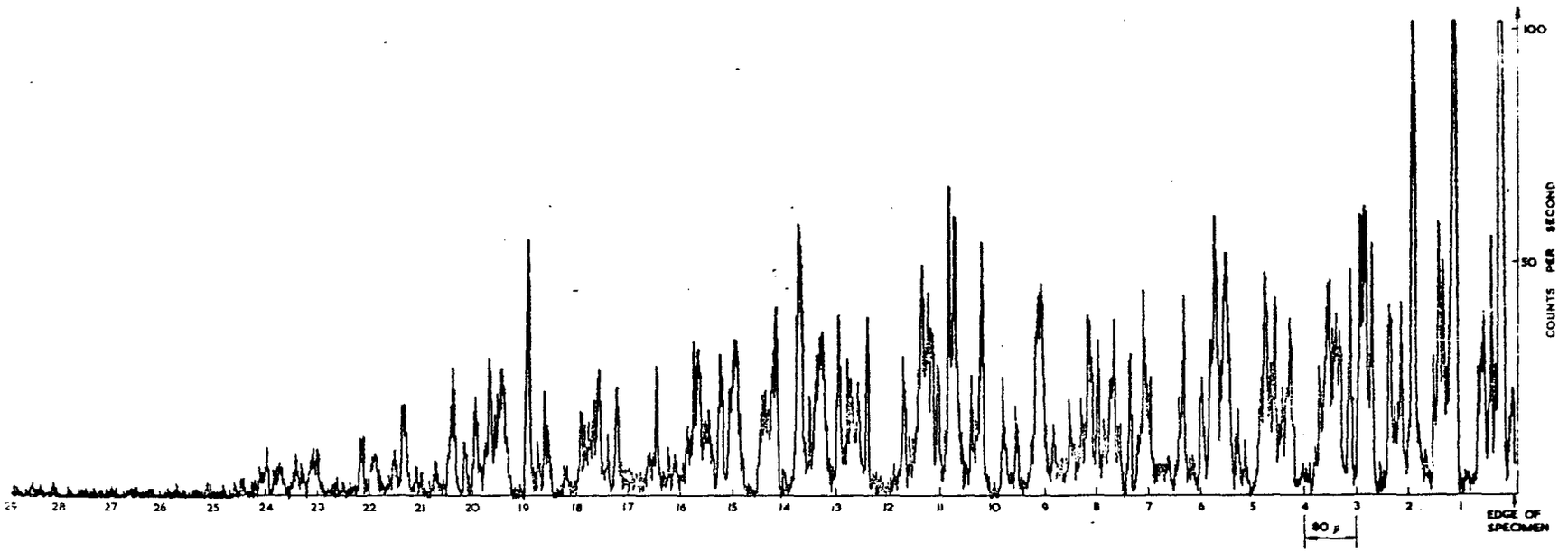

Fig 4

Microprobe recording for strontium in CYX 165 graphite at 848°C

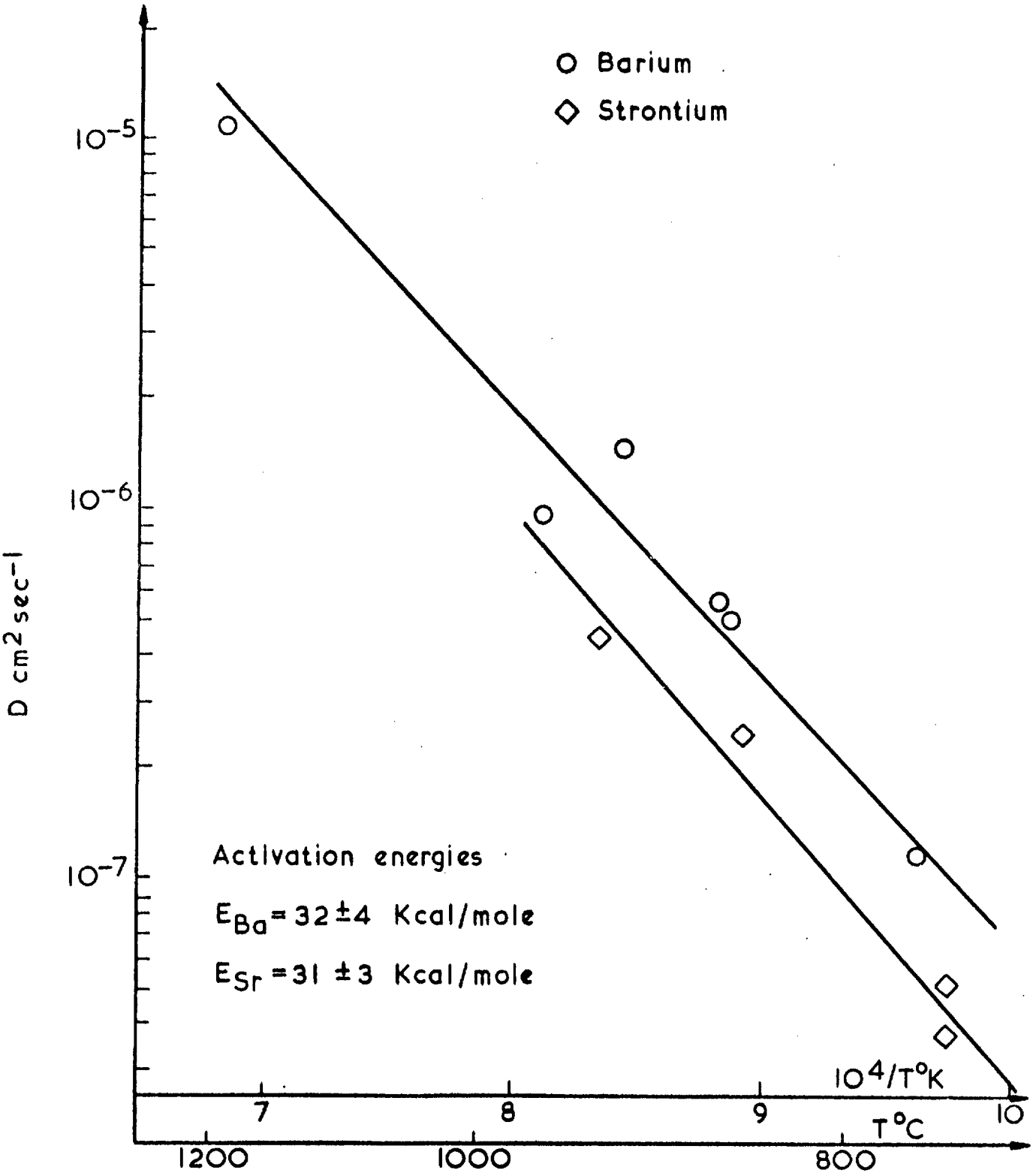

FIG. 5. ARRHENIUS PLOT FOR BARIUM AND STRONTIUM IN CY X 165 GRAPHITE

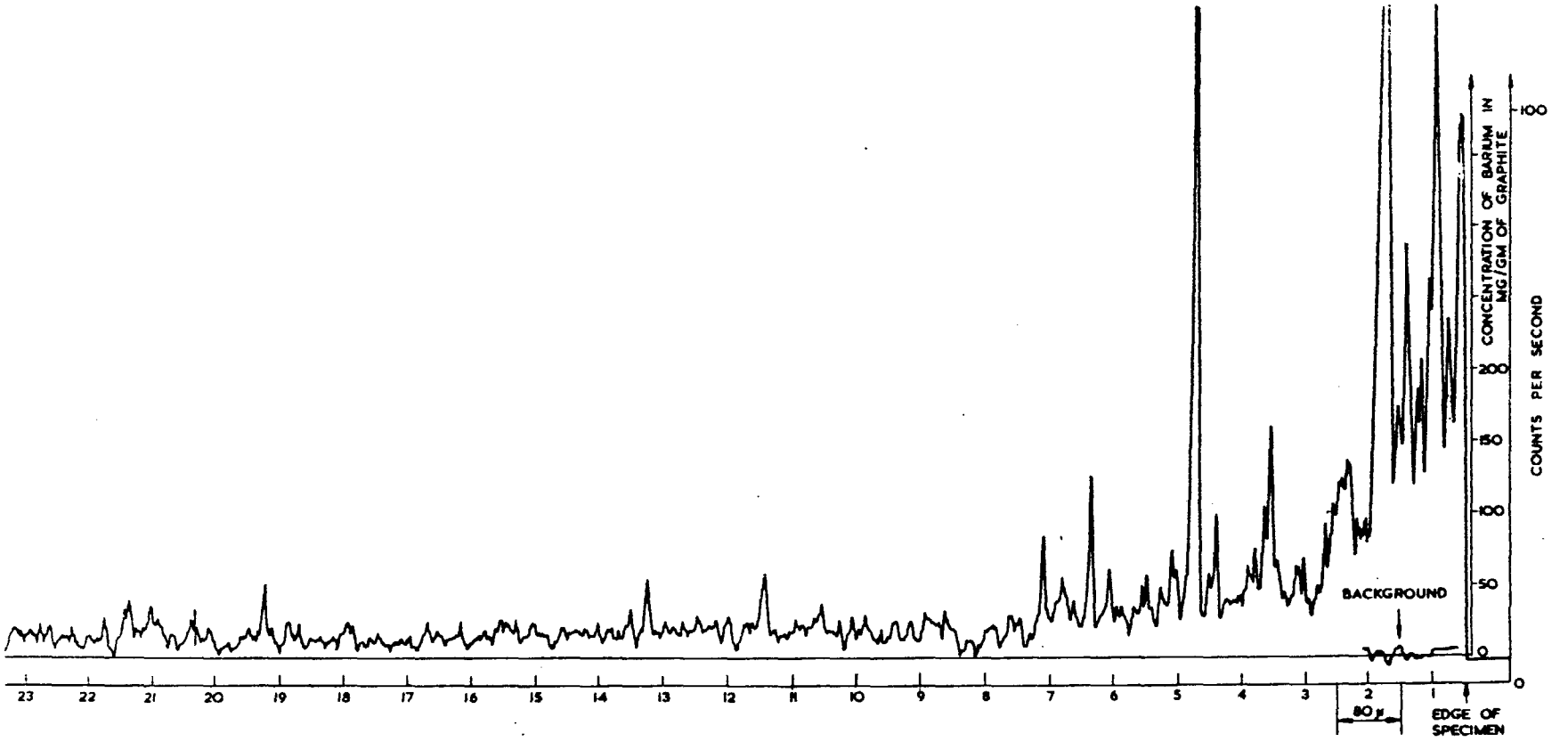

Fig 6

Microprobe recording for barium in G5 graphite at 942° C

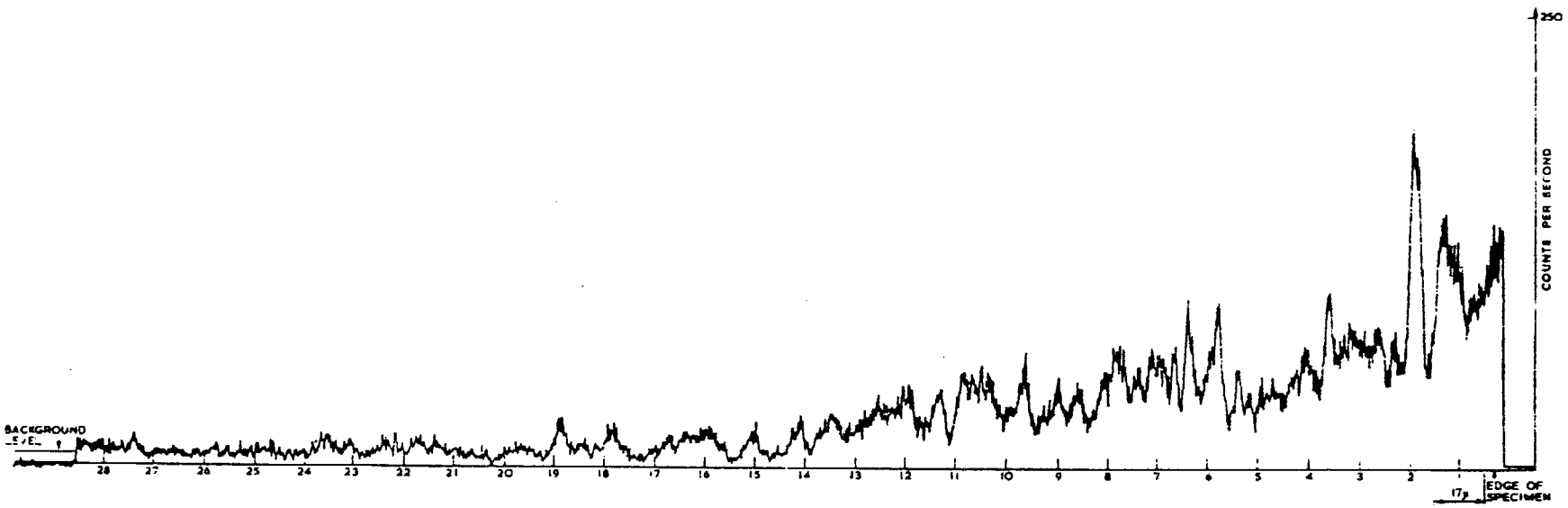

Fig 7

Microprobe recording for barium in HX 30 graphite at 858°C

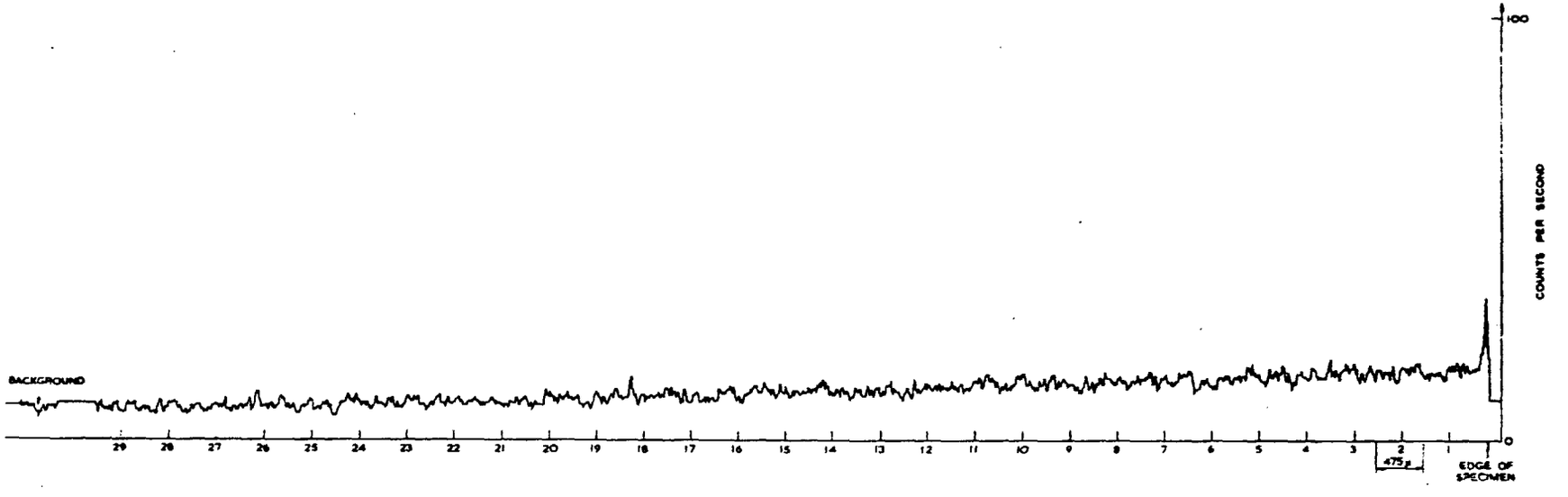

Fig 8

Microprobe recording for barium in pyrographite – "a" direction at 908°C

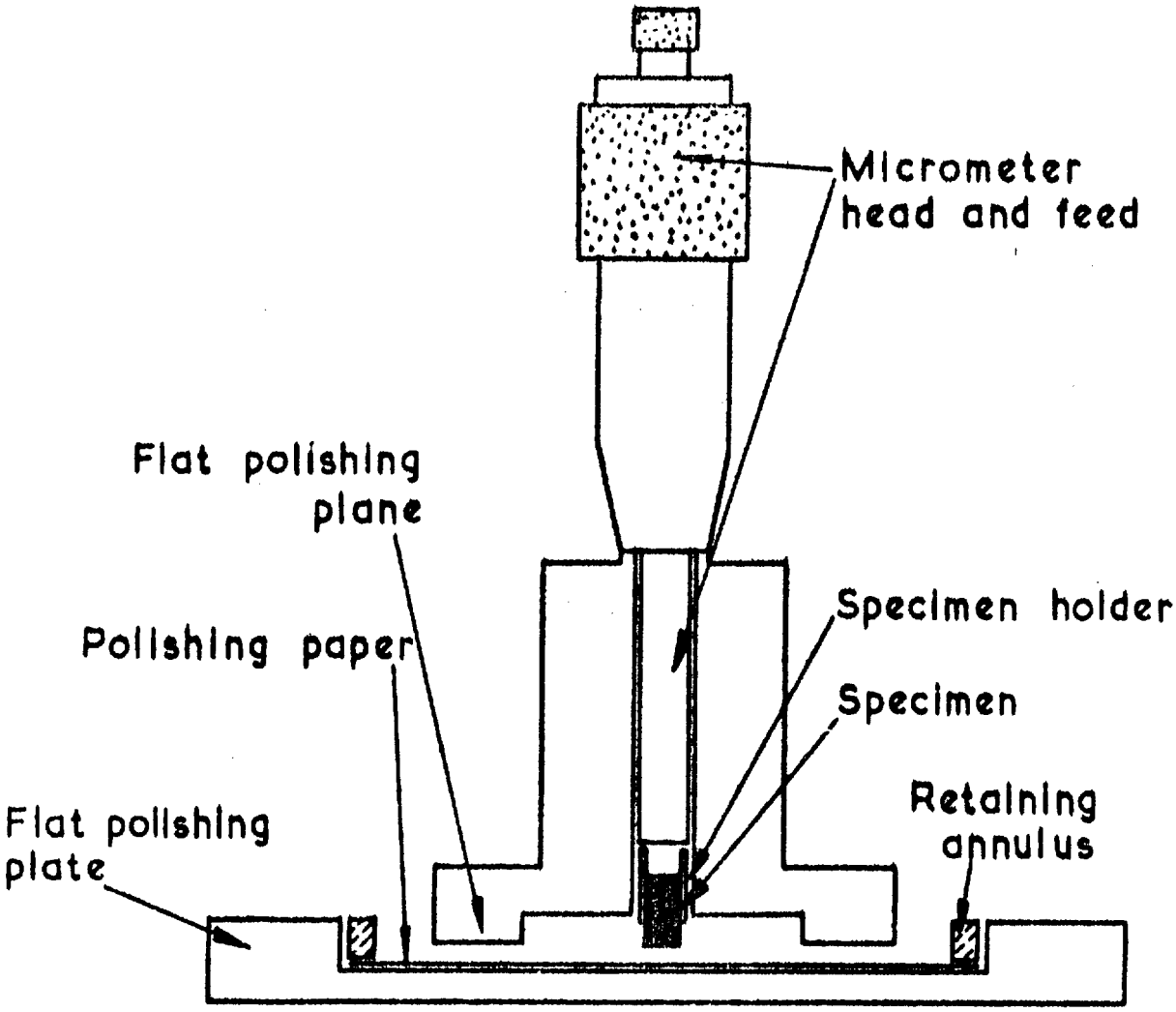

FIG. 9. SECTIONING APPARATUS

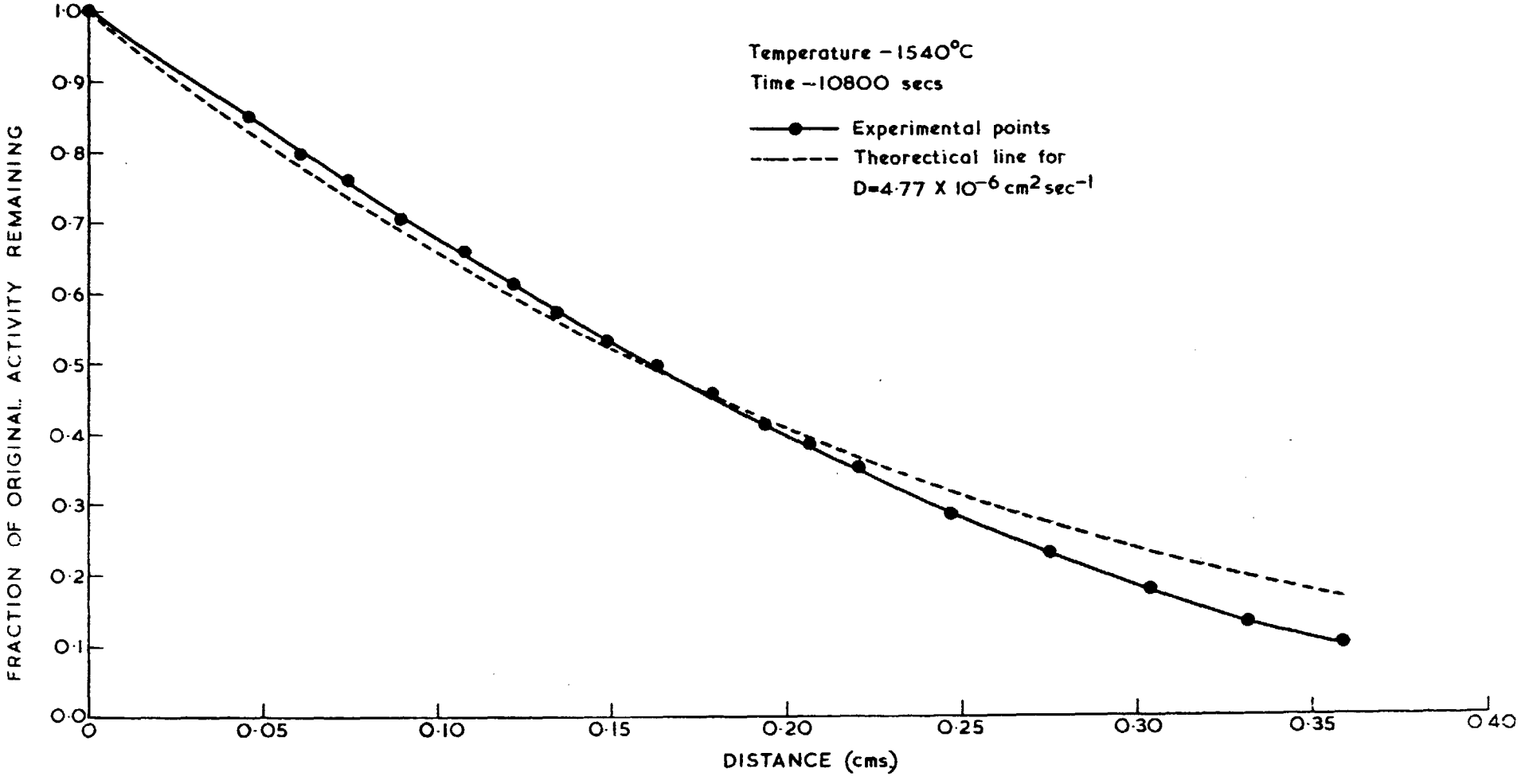

FIG. 10. PENETRATION CURVE FOR CERIUM DIFFUSION IN H X 30 GRAPHITE

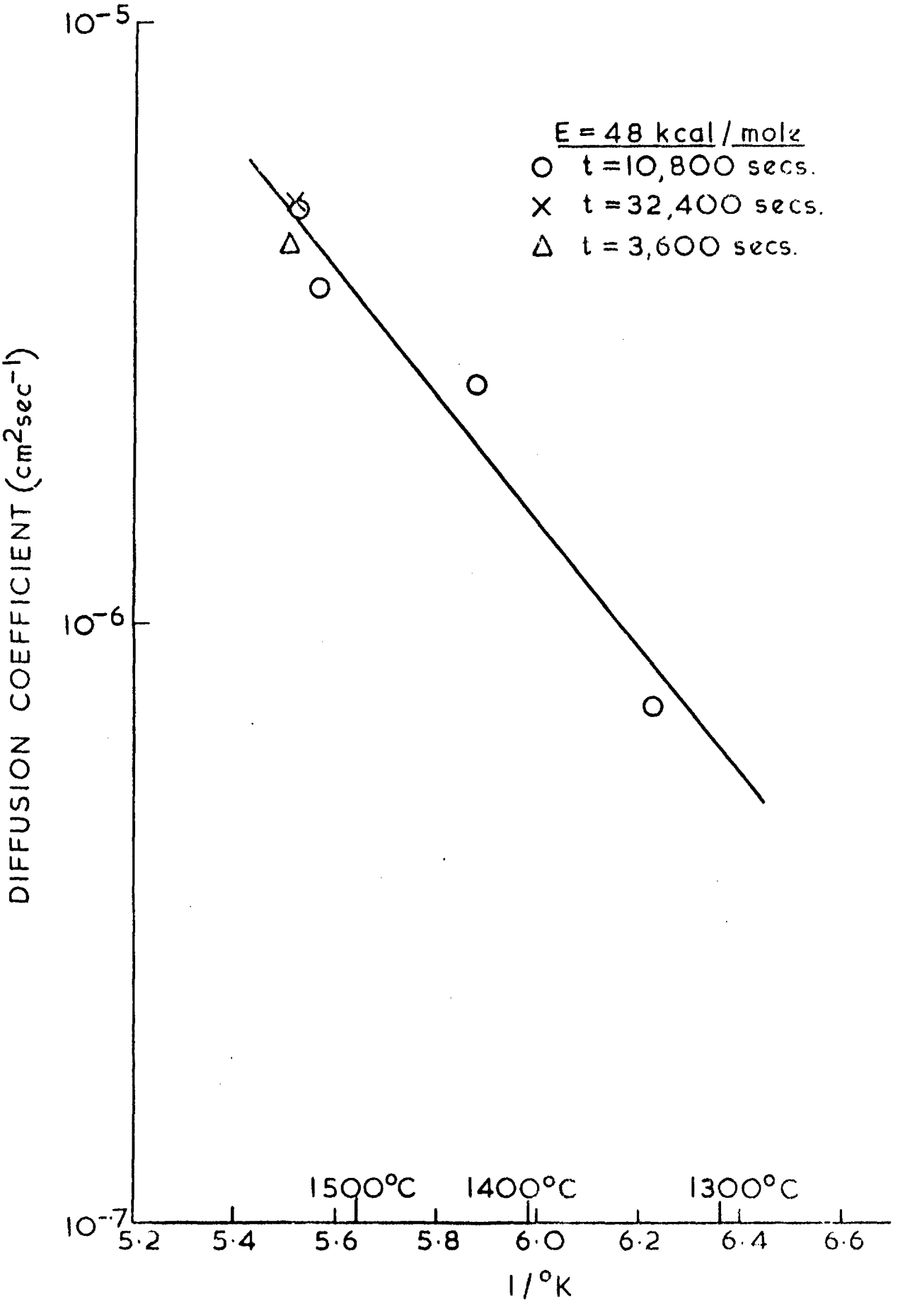

FIG. 11. ARRHENIUS PLOT FOR CERIUM DIFFUSION IN HX30 GRAPHITE